

Dealkylation in Fluid Catalytic Cracking Condition for Efficient Conversion of Heavy Aromatics to Benzene–Toluene–Xylene

Di Wang, Xiaoli Wei, Shi Shou, and Jianhong Gong*

Cite This: *ACS Omega* 2023, 8, 10789–10795

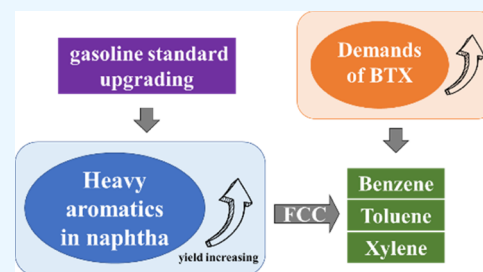
Read Online

ACCESS |

Metrics & More

Article Recommendations

ABSTRACT: Based on the characteristics of typical C_9^+ aromatics in naphtha fractions, the effects of key process parameters and heavy aromatic composition on product distribution of fluid catalytic cracking (FCC) of heavy aromatics (HAs) were investigated. The results show that catalysts with large pore size and strong acid sites are favorable for the conversion of HAs to benzene–toluene–xylene (BTX) at higher reaction temperatures and moderate catalyst–oil ratios (C/O). With a Y zeolite-based catalyst which was hydrothermally pretreated for 4 h, the conversion of Feed 1 at 600 °C and C/O of 10 may reach 64.93%. Meanwhile, the yield and selectivity of BTX are 34.80 and 53.61%, respectively. The proportion of BTX can be adjusted within a certain range. The HAs from different sources show high conversion and good BTX selectivity, which provides strong support for the technological development of HAs to light aromatics in FCC operation.



1. INTRODUCTION

Heavy aromatics (HAs) are C_9 – C_{11} aromatics with boiling points between 140 and 216 °C, and they mainly come from catalytic reforming, steam cracking, and catalytic cracking units. With the shift in chemical production patterns, more Aromatics Complex and large steam crackers are being built or expanded in refineries. At the same time, fluid catalytic cracking (FCC) is being designed to produce less fuel oil and more chemicals as the degree of cracking deepens. The above changes may lead to a continuous increase in byproduct HAs. However, the low content and difficult separation of high-value components make it difficult to effectively use HAs contained in naphtha directly. Current and future gasoline standards limit the use of HAs as a blending component.^{1–4} In recent years, the demand for benzene–toluene–xylene (BTX) has increased with the rapid growth of the petrochemical industry. Since FCC naphtha is rich in HAs, converting these HAs to BTX can make full use of HAs and thus fill the supply and demand gap for BTX.

Extensive research has been conducted in thermal hydrodealkylation, catalytic hydrodealkylation, and transalkylation. However, these technologies are often plagued by issues of economics and feedstock adaptability.⁵ Some research has been applied on cracking in the absence of hydrogen, but coke generation is always a challenge.^{6,7}

FCC, characterized by no hydrogen consumption, flexible operation, good adaptability to feedstock, low operating expense, and continuous regeneration of catalysts, is considered as an effective process to facilitate the dealkylation reaction.⁸ Based on FCC technology, HAs can be efficiently

converted to BTX with light olefins as the byproduct, which will further increase the value of HA-related products.

2. MATERIALS AND METHODS

2.1. Feedstock. Feed 1 comes from a deep catalytic cracking (DCC) unit. DCC is a catalytic cracking technology that uses heavy oil to produce light olefins. The aromatic content of its cracked naphtha is 40 to 70 wt %, with C_9^+ A accounting for 45 to 60 wt % of aromatics. Feed 2 comes from light cycle oil (LCO) to an aromatics (LTA) unit. LTA is a combined technology of selective hydrogenation of LCO and the FCC unit to produce high-octane naphtha distillates rich in aromatics. The content of aromatics in the produced naphtha is 50 to 70 wt %, with C_9^+ A accounting for 40 to 60 wt % of aromatics. Feed 3 comes from a maximizing iso-paraffin (MIP) unit. MIP is an FCC technology that maximizes the naphtha iso-paraffin content with reduced olefin content in gasoline to maintain the octane value of gasoline. The aromatic content of its gasoline products is about 20 to 40 wt %, with C_9^+ A accounting for 50 to 70 wt % of aromatics. The detailed composition of the three feeds is listed in Tables 1 and 2.

2.2. Catalysts. In this work, FCC catalysts based on Y zeolite, ZSM-5 zeolite, and BEA zeolite, which were prepared

Received: October 9, 2022

Accepted: December 30, 2022

Published: March 17, 2023



Table 1. Group Composition of Feeds

components (wt %)	feed 1	feed 2	feed 3
paraffin	13.39	13.16	19.60
olefin	3.61	0.69	2.08
naphthene	1.97	0.21	1.08
aromatic	81.04	85.94	77.23
C ₉ ⁺ A	80.21	76.92	69.99

Table 2. Composition of C₉⁺A of Feeds

components (wt %)	feed 1	feed 2	feed 3
C ₉ A			
<i>n</i> -propyl-benzene	0.49	0.11	0.26
cumene	1.86	3.26	2.27
3-methyl-ethylbenzene	14.84	14.02	11.72
4-methyl-ethylbenzene	7.59	6.41	4.66
2-methyl-ethylbenzene	4.87	4.24	3.72
1,3,5-trimethyl-benzene	7.56	6.83	6.74
1,2,4-trimethyl-benzene	27.75	19.05	21.09
1,2,3-trimethyl-benzene	6.37	3.44	4.73
indan	5.16	4.29	2.63
sum	76.49	61.65	57.83
C ₁₀ A			
butyl-benzene	0.45	0.20	0.08
methyl-propyl-benzene	3.51	4.39	4.57
diethyl-benzene	1.91	1.88	2.06
dimethyl-ethylbenzene	5.37	6.30	6.46
tetramethyl-benzene	1.96	5.19	3.38
naphthalene	0.00	2.27	8.80
methyl-indan	2.20	5.15	6.00
other C ₁₀ A	5.66	7.24	6.56
sum	21.07	32.62	37.93
C ₁₁ A			
dimethyl-indan	0.63	1.36	0.98
other C ₁₁ A	1.81	4.37	3.26
sum	2.44	5.73	4.24
total	100.00	100.00	100.00

by the same method and formula, were used. Moreover, all catalysts applied were subjected to hydrothermal pretreatment. The acid content of the catalyst was measured by NH₃-TPD

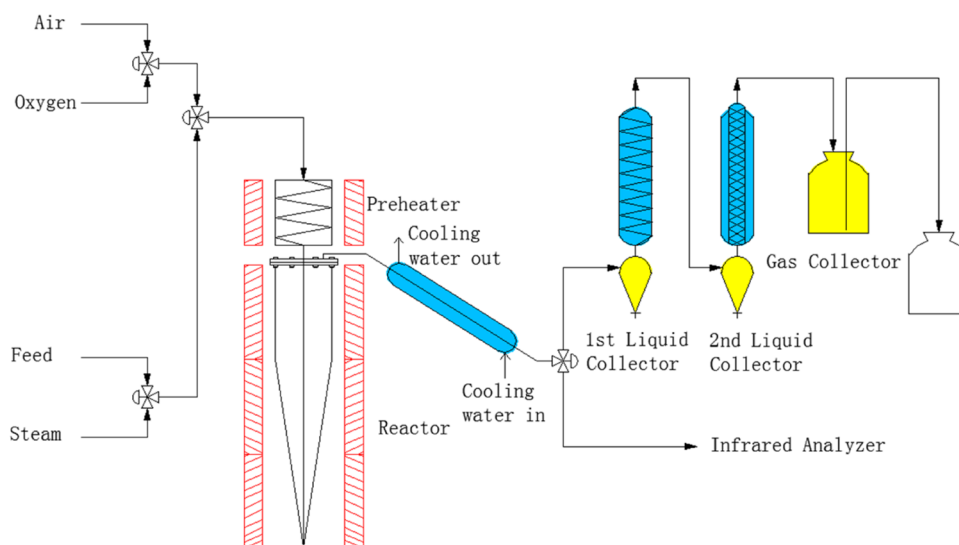
on an AutoChem II 2920 multifunctional sorbent meter from Micromeritics. The surface area and porosity were measured by static low-temperature nitrogen adsorption capacity on an AS-6B physical adsorption apparatus manufactured by Qantachorm, USA.

2.3. Experimental Process. The experiments were performed on a fixed fluidized bed (FFB) catalytic cracking reactor as shown in Scheme 1. The catalyst–oil ratio (C/O) might vary from 2 to 40. The catalyst was kept fluidized by steam. HAs entered the FFB reactor and were cracked in contact with the catalyst. The catalyst and liquid product were stripped with steam, during which the product was continuously discharged. The product was separated into a gaseous product and a liquid product by a cooling system. The gaseous products were collected and quantified by drainage collection. The liquid product collected from the two liquid collectors was analyzed after mixing. A refrigerant in the first and second stage condensate tubes was room temperature water. In the third stage condenser tube, there was $-8\text{ }^{\circ}\text{C}$ glycol, which condensed the C₅⁺ component into a liquid product. After 30 min of stripping, regeneration of the catalyst began with 2 L/min O₂ at 680 °C for 20 min. Each experiment under the same condition was repeated twice.

2.4. Product Analysis. Gaseous products were analyzed on a gas chromatograph (GC) equipped with a flame ionization detector (FID) and a thermal conductivity detector. Liquid products and the feeds were analyzed on a GC equipped with the FID detector and a PONA capillary column (100 m × 0.25 mm × 0.5 μm). The coke content was calculated using a CO and CO₂ analyzer at the flue gas outlet. In this work, the mass balance was based on the sum of gaseous, coke, and liquid products. The mass balances for all experiments exceeded 97 wt %, and the error of the repeated experiments was less than 1%.

3. RESULTS AND DISCUSSION

3.1. Characteristics of Feed Composition. HAs from various sources tend to have different compositions. According to Table 2, the C₉A content of the three HAs is the highest among all aromatics. The C₉A content of Feed 1 is the highest among the three HAs, reaching more than 77%. C₉⁺A in Feed

Scheme 1. Schematic Diagram of a Fixed Fluidized Catalytic Cracking Bed Unit

3 has the lowest C_9A content of about 57%. Among C_9A , trimethylbenzene (TMB) has the highest content, followed by methyl ethylbenzene (MEB). In C_9^+A of Feed 1, the sum of TMB and MEB contents accounts for about 69% of the total C_9^+A . In C_9^+A of Feeds 2 and 3, the corresponding values are lower about 54 and 53%, respectively. The content of dimethyl-ethylbenzene in C_{10} aromatics is relatively high. The composition of C_9^+A suggests a higher content of aromatics containing multiple short side chains in naphtha HAs. The shorter the side chain, the higher the energy of the C–C bond to be overcome for dealkylation. Therefore, there is a great need to explore methods to facilitate the dealkylation of HAs with multiple short side chains.

The kinetic diameters of C_9A were calculated by Gaussian 09. The structural optimization on the model compounds was based on the theory level of B3LYP/6-31g(D,P). The length, width, height, and kinetic diameters of C_9A were further analyzed by Multiwfn. As shown in Figure 1, the kinetic diameter of C_9A ranges from 0.69 to 0.90 nm.

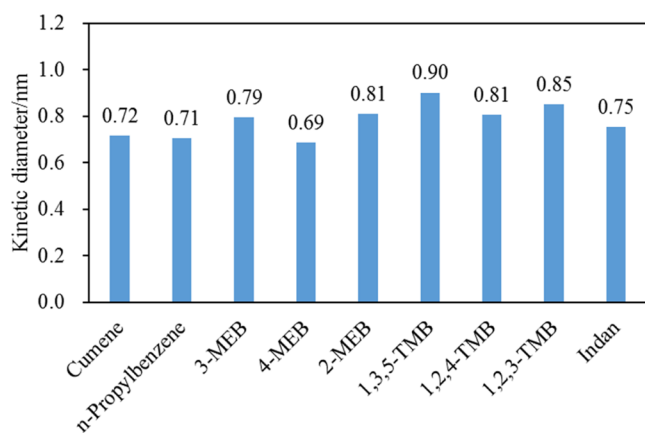


Figure 1. Kinetic diameter of C_9A .

3.2. Influence of Catalyst Properties. **3.2.1. Catalyst Characterization.** The surface area and pore volume of the three catalysts are listed in Table 3, and the acid content is shown in Figure 2.

Table 3. Properties of Catalysts Based on Different Zeolites

item	zeolites contained in catalysts		
	Y	BEA	ZSM-5
BET surface area (m^2/g)	116.20	143.98	180.90
<i>t</i> -plot micropore area (m^2/g)	44.29	86.15	110.80
<i>t</i> -plot external surface area (m^2/g)	71.90	57.83	70.10
pore volume (cm^3/g)	0.16	0.18	0.17
<i>t</i> -plot micropore volume (cm^3/g)	0.02	0.04	0.05
adsorption average pore width (nm)	5.5	5.07	3.78

3.2.2. Influence of Catalyst Properties. The effect of zeolite type was studied based on the catalytic cracking of Feed 1 evaluated at 600 °C. According to Figure 3a, the reactivity of the catalyst based on Y zeolite is higher than those of the catalysts based on BEA and ZSM-5 zeolites. In addition, $C_{11}A$ was the most reactive, probably as a result of the paring reaction.⁹

In Figure 3c, the conversions of C_9A and $C_{10}A$ are basically the same. According to Figure 3b, in C_9A , the dealkylation of

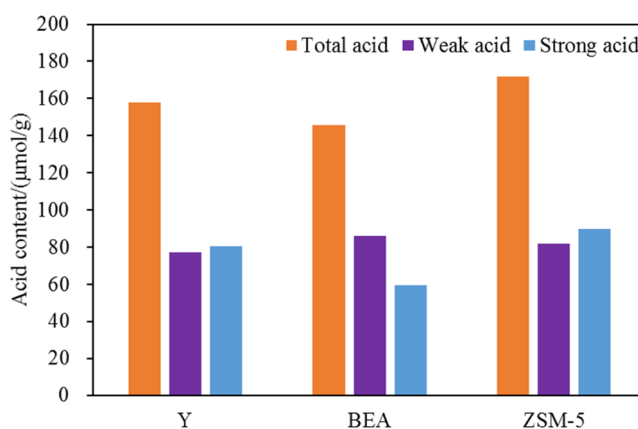


Figure 2. Acidity of catalysts based on different zeolites.

methyl is usually more difficult than those of ethyl and propyl.^{10,11} The conversion of Feed 1 reaches 53.97 wt % with the catalyst based on Y zeolite, while it is only 16.10 wt % with the catalyst based on ZSM-5 zeolite. The large difference in the conversion of TMB between the catalysts based on Y zeolite and ZSM-5 zeolite can be explained by their skeletal structures. ZSM-5 zeolite possesses linear channels of 0.53 nm \times 0.56 nm and meandering channels of 0.51 nm \times 0.55 nm.¹² Due to the large kinetic diameters of HAs as shown in Figure 1, cracking occurs mainly on the outer surface of ZSM-5, where there are fewer acid sites, which limits the conversion of HAs. In contrast, Y zeolite has a channel diameter of 0.74 nm and has a unique super cage structure.^{13,14} As a result, larger aromatic molecules, such as TMB and MEB, can diffuse into the internal micropores of Y zeolites.

BEA zeolite has a larger channel of 0.57 nm \times 0.75 nm but a lower acidity and weaker acid strength.^{15,16} Experiments showed that Feed 1 has a low conversion of 15.98 wt % over the catalyst based on BEA zeolite. Although a higher product yield can be achieved over the catalyst based on Y zeolite, the catalysts based on BEA and ZSM-5 zeolite show approximately equal selectivity for BTX as the catalyst based on Y zeolite. Due to the fact that the conversion of C_9^+A is well adapted to different zeolites, there is a great opportunity to integrate or couple the conversion of HAs with various common catalytic cracking technologies.

In addition to the differences in conversion, the distribution of BTX as shown in Figure 3d varies with the nature of the zeolite. The kinetic diameters of benzene, toluene, and xylene range from 0.68 to 0.76 nm. The proportions of benzene, toluene, and xylene are not affected by the shape selection of Y zeolite since the nonrigid and vibrating framework of zeolite allows the passage of molecules 0.1 nm larger than the channel diameter.¹⁷ According to the rule of parallel sequential reactions, xylene has a relatively high proportion in BTX, while benzene has the lowest one. The smaller pore size of ZSM-5 inhibits the formation and accumulation of larger molecules while allowing the production of small transition state molecules. Therefore, on the ZSM-5 zeolite-based catalyst, the proportion of toluene in BTX is higher than the corresponding value of xylene.

Since both acidity and acid strength may affect the conversion of HAs, the effect of acid properties on catalytic performance was investigated by hydrothermal deactivation. The catalyst based on Y zeolite was treated with 800 °C steam for a period of time using hydrothermal deactivation

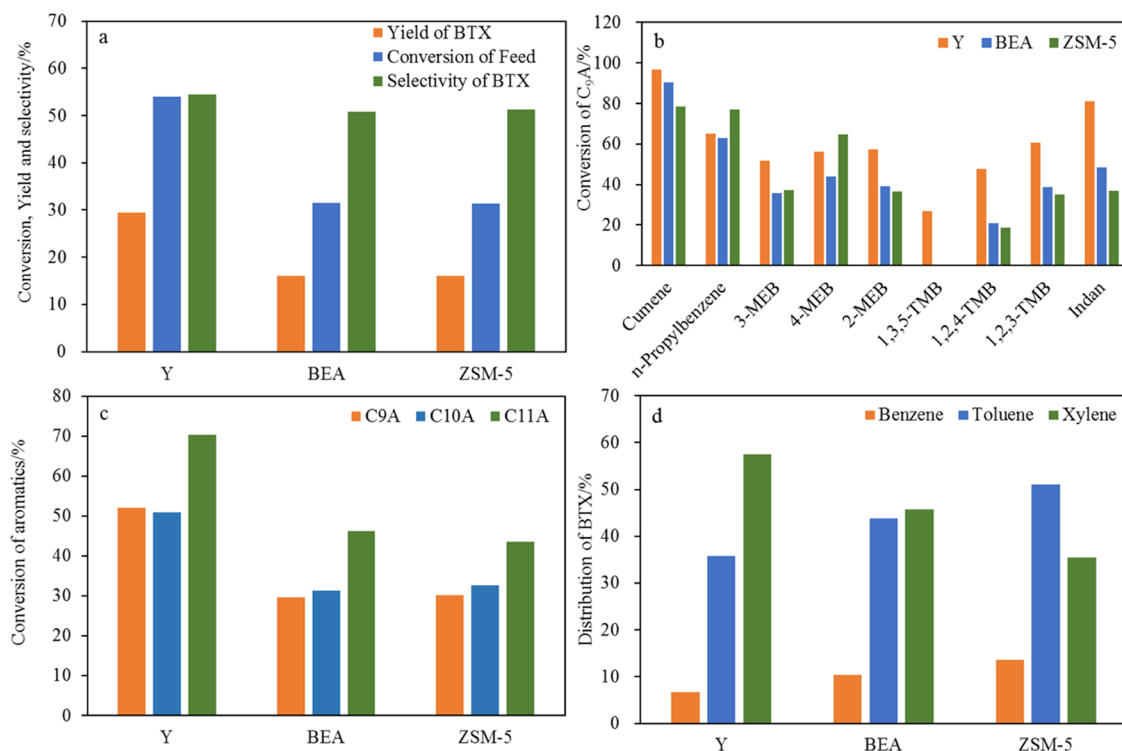


Figure 3. Conversion of Feed 1, yield, and selectivity of BTX (a–c) and distribution of BTX (d) over catalysts based on different zeolites; 600 °C and C/O of 10.

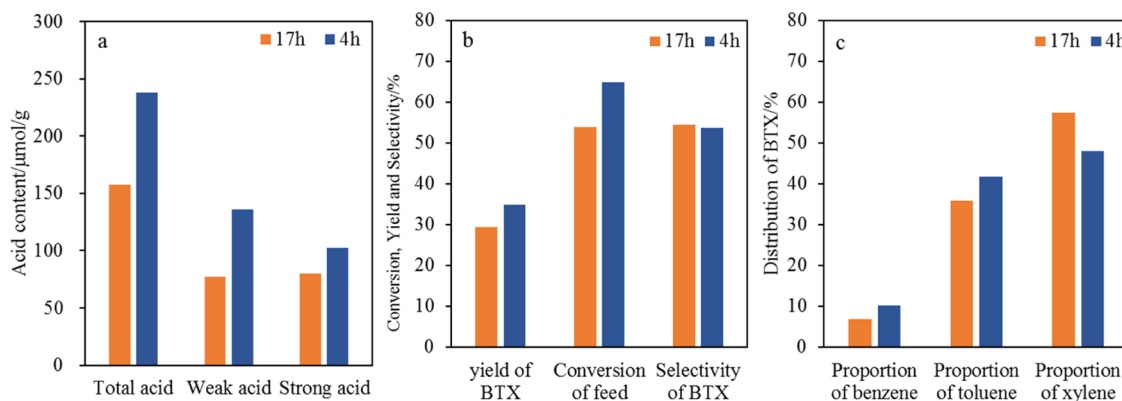


Figure 4. Acid content of catalyst with different hydrothermal treatment times (a), yield of BTX (b), and distribution of BTX (c); Feed 1, catalyst based on Y zeolite, 600 °C and C/O of 10.

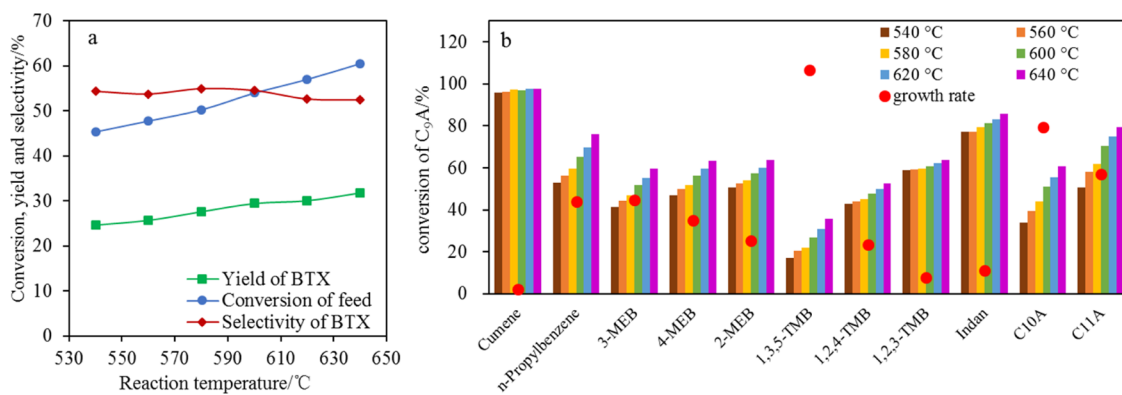


Figure 5. Conversion of Feed 1, yield, and selectivity of BTX (a) and conversion of C₉A (b) at different reaction temperatures; C/O = 10, catalyst based on Y zeolite aging for 17 h.

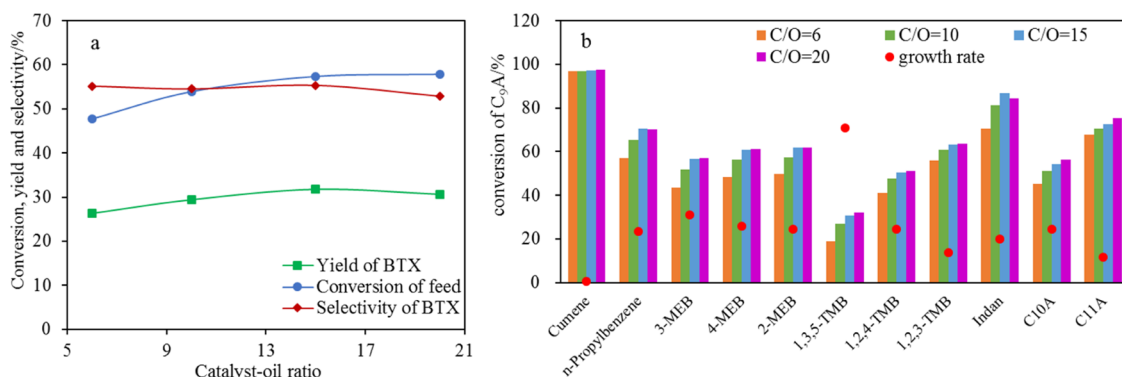


Figure 6. Conversion of Feed 1, yield, and selectivity of BTX (a) and conversion of C₉+A (b) at different catalyst–oil ratios; 600 °C, catalyst based on Y zeolite aging for 17 h.

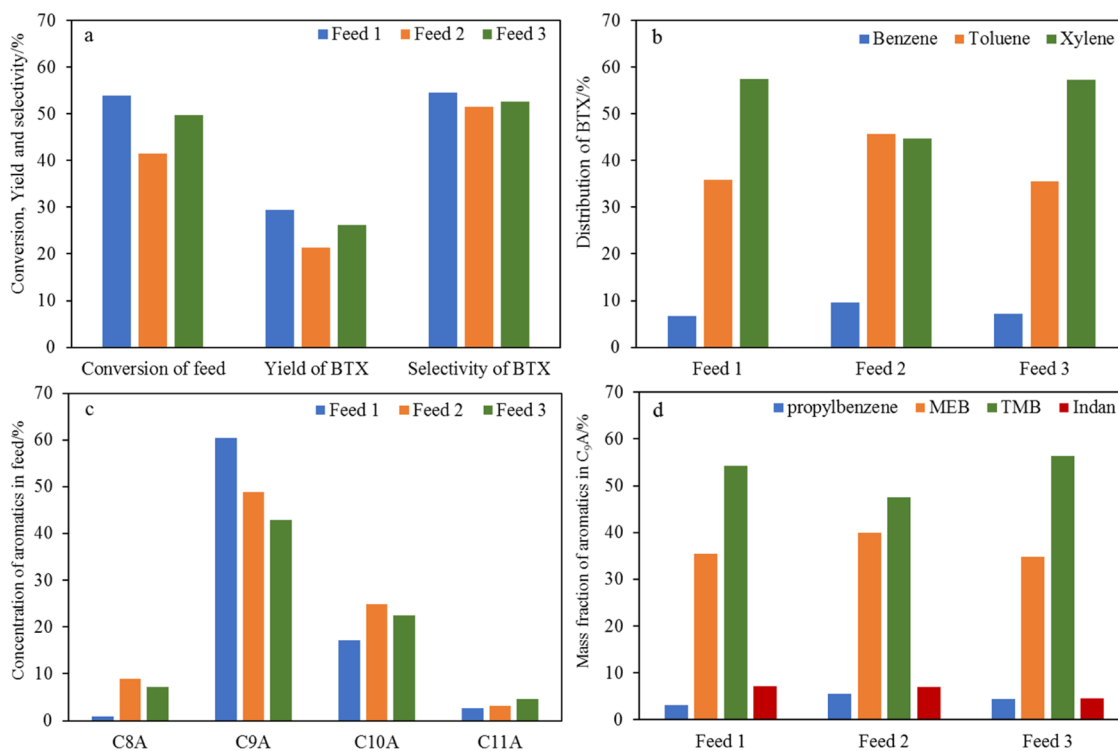
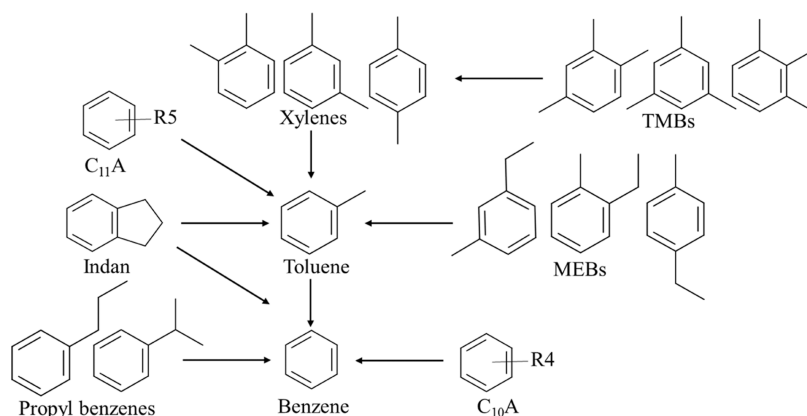


Figure 7. Conversion of feeds, yield, and selectivity of BTX (a) and distribution of BTX (b), concentration of aromatics in feeds (c, d); 600 °C, C/O = 10, catalyst based on Y zeolite aging for 17 h.

equipment. When the hydrothermal deactivation time of the catalyst is extended, the conversion of HAs and the yield of BTX decrease. Nevertheless, there is little change in the selectivity of BTX as shown in Figure 4b. According to Figure 4c, the proportion of benzene and toluene increases but the proportion of xylene decreases as the hydrothermal treatment time is shortened. The above trend stems from the fact that more TMB is converted to xylene and more xylene is converted to toluene when acidity and acid strength increase. Meanwhile, more MEB is converted to toluene.¹⁸ However, the conversion of toluene to benzene is less likely to occur than the conversion of xylene to toluene, resulting in an increase in the toluene proportion. Thus, a longer hydrothermal treatment time is not favorable for the conversion of HAs to light aromatics. Also, the conversion rate of xylenes to benzene and toluene is reduced.

In summary, to promote the conversion of HAs, zeolites with large pores and strong activity should be selected. The proportion of BTX can be adjusted within a certain range.

3.3. Influence of Reaction Conditions. Reaction temperature is one of the key factors affecting the cracking performance. Figure 5a shows that the conversion of Feed 1 increases from 45.32 to 60.53% as the reaction temperature increases from 540 to 640 °C. The selectivity of BTX does not change much at the reaction temperature between 540 and 580 °C but shows a decreasing trend after 580 °C. At a reaction temperature ranging from 540 to 640 °C, the selectivity of BTX is between 50 and 55%. As the reaction temperature increases, the BTX yield increases from 24.63 to 31.79%, an increase of about 7%. To improve the conversion of HAs and increase the yield of BTX, a relatively high reaction temperature can be chosen. However, if the reaction temperature is too high, the selectivity of BTX will decrease due to the increase in the yield of byproducts such as coke.^{19,20}

Scheme 2. Proposed Reaction Network of C_9^+A Conversion

With the increase in reaction temperature, the conversion of C_9^+A increases to different degrees as shown in Figure 5b. Among them, $C_{10}A$ and 1,3,5-TMB show the largest increase in conversion, followed by $C_{11}A$, *n*-propyl benzene, and 3-MEB. Increasing the reaction temperature shows little benefit to the yields of cumene and indan due to their high conversion.

In FCC operation, the *C/O* value is also an important parameter that affects cracking performance. Figure 6a shows that the conversion of Feed 1 increases from 47.82 to 57.90% as the *C/O* increases from 6 to 20. The above results can be attributed to the fact that the increase in *C/O* provides more active sites for the reaction, thus promoting cracking. At the same time, the yield of BTX increases, reaching a maximum value of 31.76% at a *C/O* of 15. The selectivity of BTX is higher than 50% in the adopted *C/O* range. The selectivity of BTX is less affected by the increase in *C/O* when the *C/O* is between 6 and 15. However, the selectivity of BTX decreases at the *C/O* higher than 15, which may be due to the occurrence of side reactions, such as coke formation, promoted by excess active sites. To maximize the yield of BTX, the *C/O* should be controlled within a reasonable range.

With the increase in *C/O*, the conversion of C_9^+A increases to different degrees as shown in Figure 6b. Among them, the conversion of 1,3,5-TMB increases the most. The conversion of other C_9^+A increases at about the same rate, except for cumene.

3.4. Influence of HA Composition. The sources of HAs are becoming increasingly abundant, and their compositions are changing considerably. Three different HAs were selected to evaluate their cracking behavior. Figure 7a shows that Feed 1 has the highest conversion rate, followed by Feed 3, which is also true for the yield of BTX. It is noteworthy that the BTX selectivity is essentially the same for the three feeds. That is to say, the upgrading of HAs by catalytic cracking has good feedstock adaptability, which facilitates the conversion of HAs from different sources in the catalytic cracking unit. In addition to the difference in conversion, the proportions of benzene, toluene, and xylene are different as shown in Figure 7b. For Feeds 1 and 3, the highest content of xylenes is observed, followed by toluene. As for Feed 2, the content of toluene and xylene is essentially the same, while the proportion of benzene is higher than that in the BTX of Feeds 1 and 3. The above results can be attributed to the properties of different feeds. Feed 2 has a higher proportion of MEB, which tends to cleave its ethyl group and produces toluene as shown in Scheme 2.²¹ At the same time, Feed 2 has a higher content of $C_{10}A$, which

prefers to undergo a paring reaction to produce benzene.^{9,22} By producing more benzene and toluene and less xylene, the proportion of xylene in the BTX of Feed 2 is reduced.

4. CONCLUSIONS

Methods to promote the dealkylation of shorter side chains of HAs in catalytic cracking were discussed in terms of both catalyst properties and reaction conditions. Due to the high bond energy of short side chains and large kinetic diameters of HAs, catalysts based on Y zeolites with strong acid sites are more suitable for the dealkylation of HAs and the production of BTX. The proportions of benzene, toluene, and xylene can be adjusted within a certain range. The proportion of benzene, toluene, and xylene in BTX varies from 6.72 to 13.54, 35.85 to 51.06, and 35.40 to 57.45%, respectively. The higher reaction temperature and moderate *C/O* ratio facilitate the conversion of HAs to BTX. With a Y zeolite-based catalyst hydrothermally treated for 4 h, and under the optimal reaction conditions at 600 °C and *C/O* of 10, the conversion of Feed 1 may reach 64.93%, with the yield and selectivity of BTX of 34.80 and 53.61%, respectively. Despite the different sources and compositions, the high conversion of HAs and selectivity of BTX in the dealkylation reaction provide strong support for the technological development of converting HAs to light aromatics in FCC operation.

■ AUTHOR INFORMATION

Corresponding Author

Jianhong Gong – Sinopec Research Institute of Petroleum Processing Co., Ltd., Beijing 100083, China; Phone: 8610-8236-9201; Email: gongjh.ripp@sinopec.com

Authors

Di Wang – Sinopec Research Institute of Petroleum Processing Co., Ltd., Beijing 100083, China; orcid.org/0000-0001-7502-0354

Xiaoli Wei – Sinopec Research Institute of Petroleum Processing Co., Ltd., Beijing 100083, China

Shi Shou – Sinopec Research Institute of Petroleum Processing Co., Ltd., Beijing 100083, China

Complete contact information is available at:

<https://pubs.acs.org/10.1021/acsomega.2c06507>

Author Contributions

D.W. and X.W.: Conceptualization; D.W. and X.W.: validation; D.W.: investigation; J.G.: resources; D.W.: data curation;

D.W.: writing—original draft preparation; S.S.: writing—review and editing; D.W. and S.S.: visualization; J.G.: supervision; J.G.: project administration. All authors have read and agreed to the published version of the manuscript.

Notes

The authors declare no competing financial interest.

ACKNOWLEDGMENTS

This work was supported by China Petroleum & Chemical Corporation (SINOPEC, No. 118004-2).

REFERENCES

- (1) Ali, S. A.; Aitani, A. M.; Ercan, C.; Wang, Y.; Al-Khattaf, S. Conversion of Heavy Reformate into Xylenes over Mordenite-based Catalysts. *Chem. Eng. Res. Des.* **2011**, *89*, 2125–2135.
- (2) Tsai, T.-C.; Liu, S.-B.; Wang, I. Metal Supported Zeolite for Heavy Aromatics Transalkylation Process. *Catal. Surv. Asia* **2009**, *13*, 94–103.
- (3) Tsai, T.-C.; Chen, W.-H.; Liu, S.-B.; Tsai, C.-H.; Wang, I. Metal Zeolites for Transalkylation of Toluene and Heavy Aromatics. *Catal. Today* **2002**, *73*, 39–47.
- (4) Al-Khattaf, S. S.; Ali, S. A.; Osman, M. S.; Aitani, A. M. Influence of Toluene–tetramethylbenzene Transalkylation on Heavy Aromatics Conversion to Xylenes. *J. Ind. Eng. Chem.* **2015**, *21*, 1077–1088.
- (5) Kong, D.; Qi, X.; Zhu, Z.; Yang, W.; Xie, Z. Technological Advances in Conversion of Heavy Aromatics to Light Aromatics. *Chem. Ind. Eng. Prog.* **2006**, *25*, 983–987.
- (6) Mobil Oil Corporation. ZSM-5/ZSM-12 Catalyst Mixture for Cracking Alkylbenzenes. U.S. Patent US4,577,050, 1986.
- (7) Mobil Oil Corporation. ZSM-5/ZSM-12 Catalyst Mixture for Cracking Alkylbenzenes. U.S. Patent US4,593,136, 1986.
- (8) Miao, P.; Zhu, X.; Zhou, Z.; Feng, X.; Miao, J.; Hou, C.; Li, C. Combined Dealkylation and Transalkylation Reaction in FCC Condition for Efficient Conversion of Light Fraction Light Cycle Oil into Value-added Products. *Fuel* **2021**, *304*, No. 121356.
- (9) Röger, H. P.; Böhringer, W.; Möller, K. P.; O'Connor, C. T. Rediscovery of the Paring Reaction: the Conversion of 1,2,4-trimethylbenzene over HZSM-5 at Elevated Temperature. In *Studies in Surface Science and Catalysis*; Elsevier, 2000; Vol. 130, pp 281–286.
- (10) Best, D.; Wojciechowski, B. W. On Identifying the Primary and Secondary Products of the Catalytic Cracking of Cumene. *J. Catal.* **1977**, *47*, 11–27.
- (11) Corma, A.; Wojciechowski, B. W. The Catalytic Cracking of Cumene. *Catal. Rev.* **1982**, *24*, 1–65.
- (12) Storck, S.; Bretinger, H.; Maier, W. F. Characterization of Micro- and Mesoporous Solids by Physisorption Methods and Pore-size Analysis. *Appl. Catal., A* **1998**, *174*, 137–146.
- (13) Wei, X. W. C.-G. Reaction Pathways and Influence of Parameters on Benzene Formation During Catalytic Cracking of Cumene. *Pet. Process. Petrochem.* **2008**, *39*, 41–45.
- (14) Tang, T.; Zhang, L.; Dong, H.; Fang, Z.; Fu, W.; Yu, Q.; Tang, T. Organic Template-free Synthesis of Zeolite Y Nanoparticle Assemblies and Their Application in the Catalysis of the Ritter Reaction. *RSC Adv.* **2017**, *7*, 7711–7717.
- (15) Pham, T. C. T.; Kim, P. S.; Yoon, K. B. Growth of Uniformly Oriented Silica MFI and BEA Zeolite Films on Substrates. *Science* **2011**, *334*, 1533–1538.
- (16) Toppi, S.; Thomas, C.; Sayag, C.; Brodzki, D.; Le Peltier, F.; Travers, C.; Dj'ega-Mariadassou, G. Kinetics and Mechanisms of n-Propylbenzene Hydrodealkylation Reactions over Pt(Sn)/SiO₂, and (Cl-)Al₂O₃. *J. Catal.* **2002**, *210*, 431–444.
- (17) Liu, Y.; Gao, Z. Molecular Dimension and Shape Selectivity of Zeolite Molecular Sieves. *Acta Pet. Sin., Pet. Process. Sect.* **1996**, *12*, 35–40.
- (18) Al-Khattaf, S.; Tukur, N. M.; Al-Amer, A.; Al-Mubaiyedh, U. A. Catalytic Transformation of C7–C9 Methyl Benzenes over USY-based FCC Zeolite Catalyst. *Appl. Catal., A* **2006**, *305*, 21–31.
- (19) Thakur, R.; Barman, S.; Gupta, R. K. Kinetic Investigation in Transalkylation of 1,2,4 Trimethylbenzene with Toluene over Rare Earth Metal-Modified Large Pore Zeolite. *Chem. Eng. Commun.* **2017**, *204*, 254–264.
- (20) Akhtar, M. N.; Tukur, N. M.; Al-Yassir, N.; Al-Khattaf, S.; Čejka, J. Transalkylation of Ethyl Benzene with Triethylbenzene over ZSM-5 Zeolite Catalyst. *Chem. Eng. J.* **2010**, *163*, 98–107.
- (21) Ali, S. A.; Ogunronbi, K. E.; Al-Khattaf, S. S. Kinetics of Dealkylation–transalkylation of C9 Alkyl-aromatics over Zeolites of Different Structures. *Chem. Eng. Res. Des.* **2013**, *91*, 2601–2616.
- (22) Chen, J.; Liu, Y.; Qiao, L.; Xu, Y.; Tian, H.; Lu, W.; Wu, L.; Yu, L.; Sun, G.; Wei, Y. et al. *Catalytic Cracking Process and Engineering*, 3rd ed.; Chen, J.; Xu, Y., Eds.; China Petrochemical Press: Beijing, 2015; pp 209–219.